# Nonlinear Interaction Mechanisms of Multi-scale Multi-mode MHD and Micro-turbulence in Magnetic Fusion Plasmas

Jiquan Li 1) , Y. Kishimoto 1) , Z. X. Wang 2)

1) Graduate School of Energy Science, Kyoto University, Uji, Kyoto 611-0011, Japan
2) Dalian University of Technology, Dalian 116024, China

E-mail contact of main author: lijq@energy.kyoto-u.ac.jp

**Abstract**. Direct numerical simulations of multi-scale multi-mode MHD and micro-turbulence at ion gyro-radius scale are performed based on gyrofluid model. We focus on the nonlinear evolution of both MHD magnetic island and micro-turbulence in a dynamically interacting system involving all zonal mode components. Here we report the progress on the understanding of nonlinear interaction mechanism with two remarkable findings: (1) A magnetic island seesaw oscillation with a pivot along the singular surface due to the interaction with micro-turbulence is observed. A minimal model is proposed to elucidate the seesaw mechanism. It is identified that fluctuating electromagnetic torque due to a cross-scale dynamo action produced by micro-turbulence may drive the island seesaw. (2) A novel ITG instability at short wavelengths is induced by a MHD magnetic island as a consequence of the breakdown of the frozen-in law. The new instability is identified to be characterized by a global structure propagating in the ion diamagnetic drift direction. Such mechanisms offer new insights in understanding complex nonlinear interaction among multi-scale multi-mode fluctuations.

## 1. Introduction

Complexity of anomalous transport in magnetic fusion plasmas does not only originate from various MHD activities and micro-instabilities due to complex magnetic geometry and non-homogeneity, but also results from highly nonlinear interaction among these fluctuations [1]. Recent experimental observations in tokamaks have shown some evidences. For example, ITBs are often formed along the low order rational $q$ surfaces; nonlocal transport occurs in the discharges with peripheral fueling or heating [2]. MHD activities are diagnosed accompanying with suddenly occurring small-scale fluctuations, showing the secondary excitation [3-5]. Such phenomena are speculated as a consequence of nonlinear interaction among macroscopic MHD activities and microscopic drift waves [6-14]. On the other hand, the interaction between electromagnetic (EM) and electrostatic (ES) and the related underlying mechanism are important fundamental topics in plasma physics. The ES fluctuation is mainly governed by the dynamics of electrical field and the associated flows such as the micro-turbulence. The EM one is dominated by the magnetic dynamics and the related current like the macro-scale MHD. Both fluctuations due to different instabilities may coexist generally such as the MHD modes and the ion temperature gradient (ITG) driven micro-turbulence commonly in tokamak plasmas. The interplay mechanism between such cross-scale fluctuations with different EM features is crucial to understand complex nonlinear EM phenomena and to explore energy-exchange channel in multi-scale EM turbulence.

Of particular interest are the magnetic island dynamics in a turbulent environment with micro-fluctuations and the effects of the developed magnetic island on the micro-turbulence in tokamak plasmas. On one hand, the MHD perturbation, especially with large magnetic island, may modify the equilibrium configuration so that the micro- instability is likely affected, while the island dynamics and magnetic reconnection may be changed in a turbulent environment with small-scale fluctuations. On the other hand, the interplay between ES micro- turbulence and EM MHD mode should become prominent due to highly complex nonlinearity, particularly in future fusion reactors like ITER. It may further create new nonlinear dynamics. In tokamak plasmas, the diamagnetic drift coupled with the magnetic fluctuation may cause island rotation or mode locking [15]. The major disruptions and degraded confinement are generally observed once the island rotation is locked in the plasma. The physics of the locked mode is operationally important to prevent the disruption in the present tokamaks and future reactors [16]. While the avoidance of the locked mode is a technical target [17,18], relaxing the mode locking to mitigate the disruption through utilizing nonlinear mechanism is a state-of-the-art approach for plasma control. Here we study the nonlinear interaction mechanisms of multi-scale multi-mode turbulence through direct gyrofluid simulation. The progress on new understanding of the nonlinear interaction dynamics between micro-turbulence and MHD fluctuations as well as the islands is reported.

## 2. Physical model and simulation settings

Aiming at understanding the interplay between multi-scale MHD and ion-scale turbulence, a 5-field gyrofluid model is employed to perform multi-scale simulation [11]. The results are applicable in explaining the experimental observations of MHD island dynamics in a torus. In a normalized form for the ion-scale drift wave, the gyrofluid model describing the multi-scale EM turbulence consists of the nonlinear evolution equations as follows

$$d_t n = -\partial_y \phi - \nabla_{//} \upsilon_{//} + \nabla_{//} j_{//} + D_n \nabla_\perp^2 n \quad , \tag{1}$$

$$d_t \nabla_\perp^2 \phi = (1+\eta_i)\partial_y \nabla_\perp^2 \phi + \nabla_{//} j_{//} + \mu_\perp \nabla_\perp^4 \phi \quad , \tag{2}$$

$$\beta \partial_t A_{//} = -\nabla_{//}(\phi - n) - \beta \partial_y A_{//} - \eta j_{//} \quad , \tag{3}$$

$$d_t \upsilon_{//} = -2\nabla_{//} n - \nabla_{//} T_i + \beta(2+\eta_i)\partial_y A_{//} + \eta_\perp \nabla_\perp^2 \upsilon_{//} \quad , \tag{4}$$

$$d_t T_i = -\eta_i \partial_y \phi - \tfrac{2}{3}\nabla_{//}\upsilon_{//} - \tfrac{2}{3}\sqrt{\tfrac{8}{\pi}}\left|\nabla_{//}\right| T_i + \chi_T \nabla_\perp^2 T_i \quad . \tag{5}$$

with $j_{//} = -\nabla_\perp^2 A_{//}$ , $\beta = 8\pi n_0 T_{i0} / B^2$ , $\eta_i = d \ln T_i / d \ln n$ . The operators $\nabla_\perp^2 = \partial_x^2 + \partial_y^2$ , $d_t = \partial_t + \hat{e}_z \times \nabla_\perp \phi \cdot \nabla_\perp$, and $\nabla_{//} = \partial_z + \hat{e}_z \times \nabla(A_{//0} + A_{//}) \cdot \nabla_\perp$ are expressed in slab geometry $\vec{B} = B_0 \hat{e}_z - \beta \nabla A_{//0}(x) \times \hat{e}_z$ with constant $B_0$. To manifest the mutual multi-mode interaction, two equilibrium models $B_{y1} \propto \tanh(x/\lambda_1) / \cosh^2(x/\lambda_1)$ and $B_{y2} \propto \mathrm{arcsinh}(x/\lambda_2)$ for the poloidal field are employed, probably corresponding to different $q$ profiles in tokamak plasmas. The former one can highlight the effect of the micro-turbulence on the MHD island dynamics. Meanwhile, the latter one is to emphasize the role of magnetic island in micro-fluctuation. Here $x$ is the distance deviated from the singular surface, $\lambda$ is the gradient length of axial equilibrium current. Note that near the singular surface, namely the rational surface $x = 0$, both models are reduced to the usual slab model in tokamak plasmas[19]. This model may be regarded as an integrated system describing the resistive MHD and micro-scale ITG modes. It can be explicitly shown by two reduced cases. At the ES limit, usual 3-field ITG model is derived with adiabatic electron response [20]. Contrarily, ignoring the drift wave effect can reduce to the conventional incompressible 2-field MHD model described by Eqs. (2) and (3) [21]. The multi-scale turbulence may be jointly controlled by $\eta_i$ and $\eta$.

The simulation can be performed using an initial value code [22], which solves the nonlinear evolution equations (1)-(5) in a 2-dimensional ($x$, $y$) plane perpendicular to the equilibrium magnetic field along the $z$ direction. The code is designed for solving a general 3-dimensional problem. Fourier transformation in $y$ and $z$ directions for any perturbed physical quantity is expressed as $f(x,y,z,t) \sim \sum_{m,n} f_{m,n}(x,t) \exp(i2\pi my/L_y - i2\pi n/L_z)$ with corresponding wave numbers $k_y = 2\pi m / L_y$, $k_z = 2\pi n / L_z$ and $k_{//} = 2\pi n / L_z - 2\pi m \hat{s} x / L_y$. An implicit finite difference scheme for $x$ variable is used with fixed boundary conditions at $x = \pm L_x / 2$. Reference parameter setting except for the key parameter pair $(\eta_i, \eta)$ in mixed-scale turbulence simulations is fixed as $\beta = 0.01, \hat{s} = 0.2$, $\lambda_1 = 25, \lambda_2 = 5$, $L_x = 100$, $L_y = 20\pi$, $D_n = \mu_\perp = \eta_\perp = \chi_T = 0.01$. Linear simulations show that the MHD and ITG instabilities can be excited simultaneously in a whole spectrum by properly choosing $(\eta_i, \eta)$. The ITG fluctuation is excited around the peak $k_y \rho_i \sim 0.6$ corresponding to usual ion-drift ITG mode. Meanwhile, the low mode number MHD fluctuations are unstable for $m \leq 2$. The MHD-dominated EM fluctuation tends to be typical of the drift tearing mode due to the diamagnetic drift effect. The magnetic island tends to propagate along electron diamagnetic drift direction since the normalized real frequency is positive for most unstable MHD. Hence, this modeling can be employed to investigate the direct nonlinear interaction between MHD mode and micro-instability with different driving forces.

## 3. Effects of micro-turbulence on magnetic island dynamics

First the equilibrium configuration with $B_{y1} \propto \tanh(x/\lambda_1) / \cosh^2(x/\lambda_1)$ is considered. The sheared poloidal magnetic field tends to be weak at edge region far from the singular surface, it is expected the magnetic island dynamics may be easily influenced by micro-turbulence. The direct gyrofluid simulations are mainly performed with unstable MHD and different ITG instabilities. All simulations show a common evolution history with four phases as illustrated in Figure 1. The details of the simulation have been described in [11], which emphasized the oscillatory nature of zonal flow dynamics. Here, the focus is mainly on the island dynamics.

### 3.1. Magnetic island seesaw oscillation in direct simulation

Most importantly, a pronounced magnetic island oscillation is commonly observed in the simulations, showing a dynamic quasi-steady state in Phase IV of Fig.1. An oscillatory ZF with finite frequency also occurs. The island oscillation is visualized by a movie of island evolution, and much more clearly by snapshots of the dominant magnetic flux component $m = 1$. The island oscillation occurs pivoting along the singular surface like a seesaw (referred to hereafter as an island seesaw). The common characteristics of the island seesaw are summarized as follows: (1) The magnetic island seesaw occurs only in the simulation with a full magnetic reconnection (namely, with larger tearing instability parameter $\Delta'$ [23]). (2) The averaged EM torque [24] $T_{EMy}\hat{z} = \iint_{xy} x\hat{x} \times (\vec{j} \times \vec{B})_y \, dxdy / L_x L_y$ exerted on the island by fluctuating EM force in the $y$ direction tends to oscillate in time in the quasi-steady state synchronizing with the island seesaw. (3) The zonal flow is also oscillatory with finite frequency, but

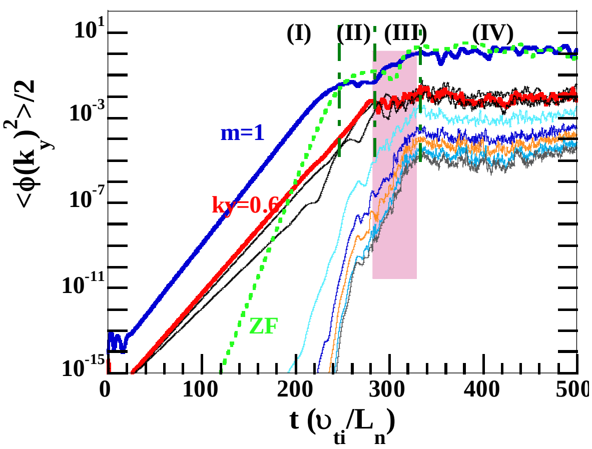


*Fig.1 Time history of kinetic energy in multi-scale MHD and ITG turbulence.* $\eta_i = 2.0$, $\eta = 5\times10^{-4}$, $\lambda_1 = 25$.

the occurrence of the island seesaw is independent of the zonal flows. (4) The EM torque and seesaw amplitude increase with increasing $\eta_i$ . (5) For smaller $\Delta'$ , the magnetic reconnection also occurs, but the island is saturated at small width, the magnetic island remains static regardless of the ITG intensity.

### 3.2. Minimal model of magnetic island seesaw mechanism

To explore the island seesaw mechanism, we here propose a minimal model, which preserves the most elementary MHD dynamics and the multi-scale interaction with ITG mode. The model consists of reduced MHD equations based on Eqs. (2) and (3) with $\psi = -A_{//}$ [23,24]

$$\partial_t \nabla_\perp^2 \phi = -[\phi, \nabla_\perp^2 \phi] + [\psi, j] \quad , \tag{6}$$

$$\beta \partial_t \psi = -[\phi, \psi] + \eta j \quad , \tag{7}$$

and an independently evolving ES ITG eigenmode [20],

$$\phi^{ITG}(t, x, k_y^{ITG}) = \hat{\phi}^{(n)}(x) e^{-i\Omega t + i k_y^{ITG} y} \quad . \tag{8}$$

The latter, representing the micro-turbulence, is involved in Poisson brackets through $\phi = \phi^{MHD} + \phi^{ITG}$. $\hat{\phi}^{(n)}(x) = H^{(n)}(\sqrt{i\sigma}x)\exp(-i\sigma x^2)$ corresponds to the complex eigenvalue $\Omega$. $\sigma$ denotes the parametric dependence, and the Hermite function $H^{(n)}$ determines the radial parity of the ITG eigenmode. Based on the kinematic dynamo theory [25,26], the level of $\phi^{ITG}$ can be artificially chosen following Eq.(8) as a given flow component considering the ITG spectral features resulting from the inverse cascade in time and space [1].

Modeling simulations are performed using the same parameters and numerical setting as in Fig.1. An island seesaw similar to that in the

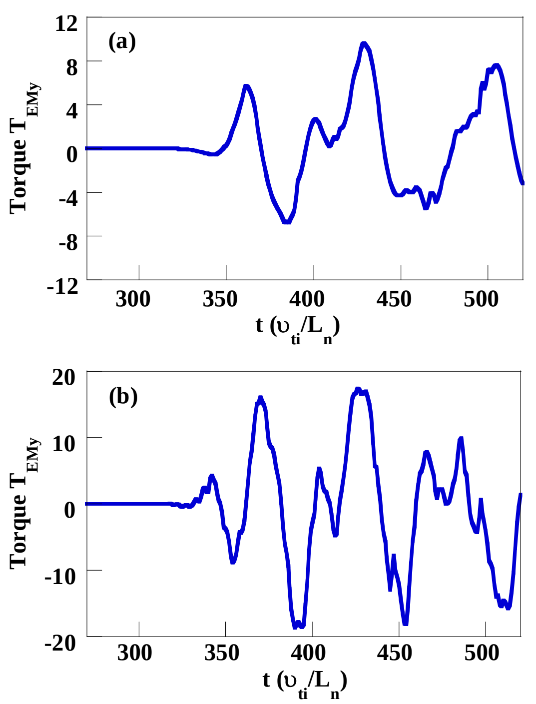


*Fig.2 Averaged EM torque (a) in modeling simulation, (b) in direct simulation.*

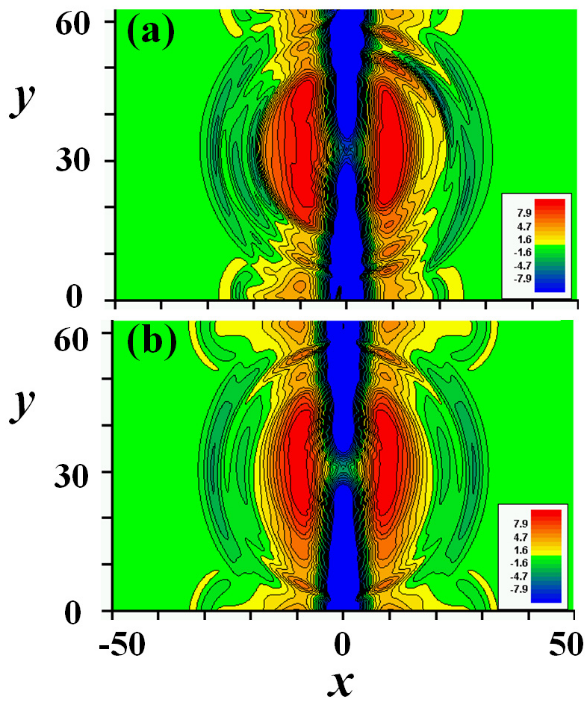


*Fig.3 Snapshots of current distribution in modeling simulations with radial (a) even-parity and (b) odd-parity ITG modes. (a) $\lambda_1 = 25$, (b) $\lambda_1 = 35$.*

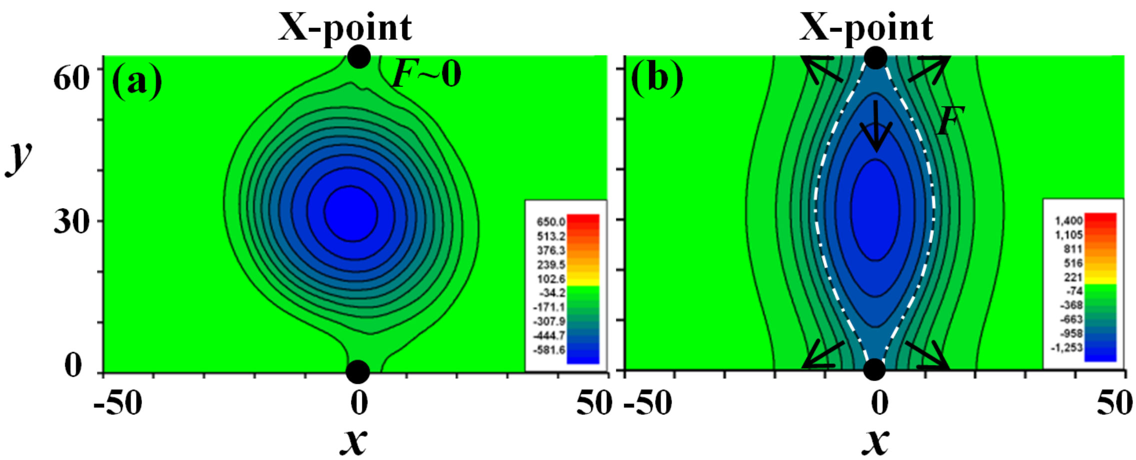


*Fig.4 Snapshots of the magnetic flux in modeling simulations of Fig.4(a) with and (b) without island seesaw. Arrows correspond to the direction of the magnetic tension force F inside and outside of the separatrix marked by the dot-dashed curve.*

direct simulations is observed only when $\phi^{ITG}$ has radial even parity. The seesaw amplitude and oscillatory EM torque increase with increasing $\phi^{ITG}$, showing the same dependence on the ITG mode as in the direct simulations. The seesaw oscillation is characterized by the real frequency $\Omega$ of the ITG mode. Note that in mixed MHD and ITG turbulence [11], the ITG spectrum connects smoothly with the MHD, showing that the ITG energy spectra are widely scattered due to nonlinear coupling. Here, we have assumed an effective ITG mode to represent whole turbulence. One multifold scan of $\Omega$, $k_y^{ITG}$, and the ITG intensity in modeling simulation shows a best-matching eigenvalue $\Omega/\omega_* \approx 0.08$ and $k_y^{ITG} = 0.3$. The corresponding $T_{EMy}\hat{z}$ is plotted in Fig.2(a), exhibiting similar behavior to that in direct simulation as shown in Fig.2(b), but with lower amplitude since the single mode was selected. A full reconnection occurs, so the island behaves like a balloon floating in the air. The underlying mechanism may be understood through the new concept of cross-scale dynamo action introduced here.

In Eq.(7), the magnetic flux responds to the interplay of the microscale $\phi^{ITG}$ through the induction term to create a dynamo current component $j_D$. The MHD flow $\phi^{MHD}$ is influenced mainly by the Maxwell stress in Eq.(6) due to the dynamo components (simulations have shown that the Reynolds stress is negligible). Note that the tearing parity is characterized by radially odd potential, denoted by $\phi^{MHD}(x) \propto \sin(k_x^{MHD} x)$ and even flux $\psi^{MHD}(x) \propto \cos(k_x^{MHD} x)$ as well as even current. Any nonlinear interaction with external flows may possibly break the MHD symmetry. If an even $\phi^{ITG}(x) \propto \cos(k_x^{ITG} x)$ is applied, the dynamo current arising from $j_D \propto \eta^{-1}[\phi^{ITG}, \psi^{MHD}]$ and the dynamo flux $\psi_D^{MHD}$ should have an odd parity based on the trigonometric function identity. The MHD potential and vorticity then involve an induced component $\phi_D^{MHD}$ and $\nabla_\perp^2 \phi_D^{MHD}$ with radially even symmetry from Eq.(6), opposed to the tearing parity. The even parity of $\phi_D^{MHD}$ signifies a positive feedback of $\phi^{ITG}$, showing a cross-scale dynamo action. The dynamo here is induced by a dynamic potential due to microturbulence, qualitatively different from those in

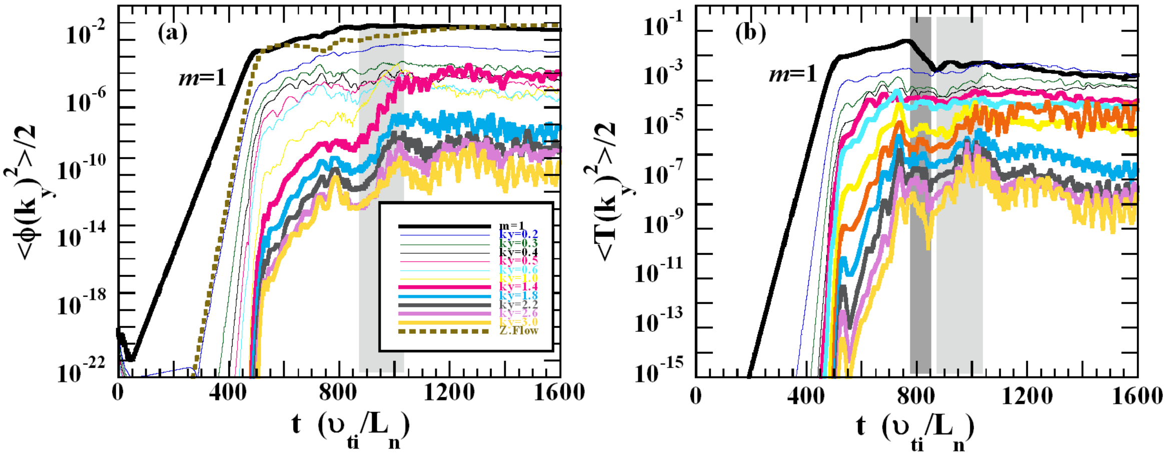


*Fig.5 Evolution of fluctuating temperature (a) and potential (b) in multi-scale direct simulation. Dark grey shaded phase in (a) marks ion temperature island collapse; the excitation of short wavelength ITG instability is light grey shaded.*

kinematic dynamo theory [25,26]. The breaking of the MHD current symmetry is visualized in Fig.3(a). If a radial odd parity $\phi^{ITG}$ is applied, all field components induced by the cross-scale dynamo action maintain the same tearing parity, as shown in Fig.3(b). The EM torques, $T_{EMy}\hat{z}$, on both sides of the singular surface have the same magnitude and almost cancel out each other owing to their opposed directions. Now it becomes clear that a dynamo current with only a radial odd-parity component may produce a non-zero oscillatory EM torque $T_{EMy}\hat{z}$ to drive the island seesaw.

Finally, the modelling simulation with small $\Delta'$ (i.e., the case with small saturated island width) is investigated. The induced EM force $\vec{j}_D \times \vec{B}^{MHD} + \vec{j}^{MHD} \times \vec{B}_D^{MHD}$ by the dynamo fields to cause the oscillatory EM torque $T_{EMy}\hat{z}$ due to the cross-scale dynamo action may be resisted by the magnetic tension force around the X-points. The latter has different directions inside and outside of the separatrix. The outside tension force can provide a component in the $y$ direction to stretch the island during the reconnection so that the island looks to be pinned between two X-points by the field lines. If the full reconnection occurs [23], the tension forces around the X-points decrease dramatically so that the island becomes “floating” in the plasma, as shown in Fig.4(a). The oscillatory EM torque can twist the floating island easily to drive a seesaw movement. Otherwise, the robust magnetic tension force out of the separatrix may persist with static island from the seesaw oscillation, as shown in Fig.4(b).

## 4. Role of magnetic island in micro-turbulence

In tokamak or stellarator, magnetic islands are commonly diagnosed with MHD activities. A natural question is how the micro-fluctuations behave in such plasmas with an island. A common argument is that the plasma is frozen in the magnetic surface [27-29] so that the driving force of micro-instability is relaxed inside the island [30,31]. To explore the response of micro-turbulence to an evolving island, our simulation is designed to have a robust MHD and weaker ITG instability in equilibrium $B_{y2} \propto \operatorname{arcsinh}(x/\lambda_2)$. Through complex nonlinear interaction similar to that in Sec.3, the multi-mode turbulence evolves to a quasi-steady state

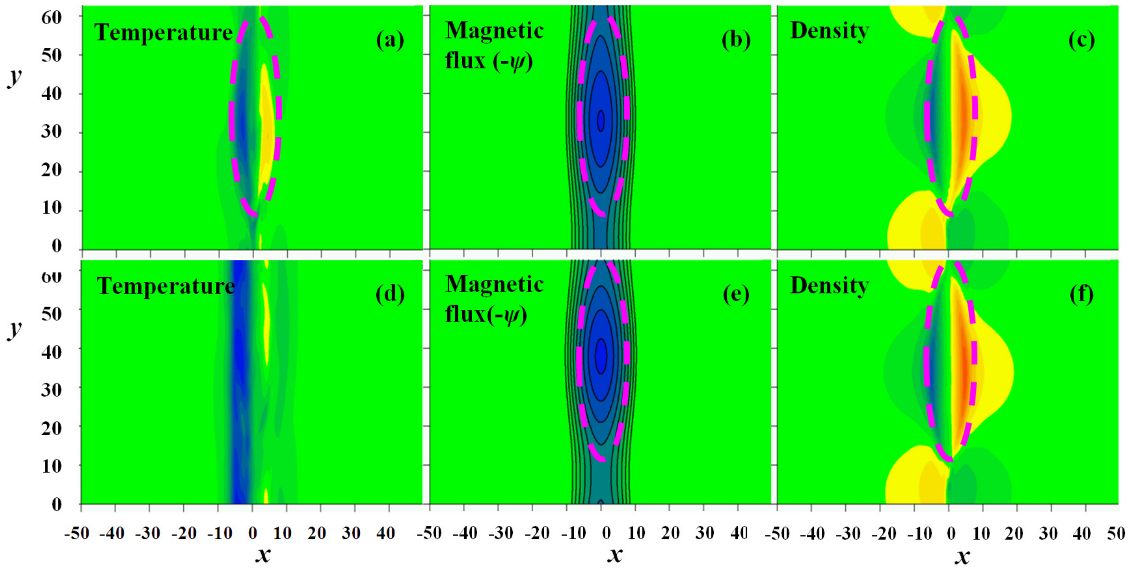


*Fig.6 Contour plots of fluctuating temperature and density and total magnetic flux (negative) before (a-c) and after (d-f) the collapse of temperature island in the simulation of Fig.5.*

dominated by MHD fluctuation. A remarkable sudden excitation of ES fluctuation with almost an identical growth rate in the quasi-steady-state at short wavelengths $k_y\rho_i \geq 1.0$ is observed after the decrease of ion temperature fluctuation as shown in Fig.5, characterized by the $m=1$ component. The magnetic component is relatively weak. The new fluctuation propagates in the ion diamagnetic drift direction surrounding the magnetic island.

To clarify the excitation mechanism of the short wavelength ITG instability, the time-evolution of all perturbed quantities and their structures are analyzed systematically in the simulation. Results show that the frozen-in condition is fairly satisfied in the early transient phase of quasi-steady-state. The magnetic island grows very slowly accompanying with gradually increasing density and ion temperature islands. This phase probably corresponds to the Rutherford stage of the nonlinear tearing mode. As the magnetic island grows to a critical width, the $m$=1 amplitude of the ion temperature fluctuation decreases sharply so that the ion temperature island collapses. The density island as well as the magnetic island still survives following the constraint of the frozen-in condition. The contour plots of the island structures before and after the collapse of ion temperature island are displayed in Fig.6. The sequence of the events shows that the ion temperature island collapse is a precondition of the secondary excitation of the short wavelength instability. Note that once the temperature island falls apart, the profile flattening inside the magnetic island under the frozen-in constraint is relieved so that the driving force of the microinstability may be enhanced. These analyses show that the short wavelength ITG instability may correspond to the magnetic island induced ITG mode, which was predicted by a preliminary linear analysis [10].

## 5. Summary

Direct numerical simulations of multi-scale multi-mode MHD and micro-turbulence at ion gyro-radius scale are performed based on gyrofluid model in slab geometry. Principal results have achieved as follows. (1) A magnetic island seesaw oscillation with a pivot along the singular surface due to the interaction with micro-turbulence. It is elucidated through a minimal model to be driven by fluctuating EM torque due to a cross-scale dynamo action. (2) A novel short wavelength ITG instability induced by a MHD magnetic island as a consequence of the breakdown of the frozen-in law. Besides possible applications to plasma transport involving the magnetic island and multi-scale EM dynamics, the island seesaw may imply a promising prototypical method for plasma disruption control in tokamaks. The major disruption may be mitigated through the relaxation of the mode locking probably by the island seesaw mechanism, suggesting a state-of-the-art nonlinear approach for plasma control. The characteristics of the new short ITG instability have been clarified. Such mechanisms offer new insights in understanding complex nonlinear interaction among multi-scale multi-mode fluctuations.

**Acknowledgements**

This work was supported by the Grant-in-Aid from JSPS (No. 19560828).

**References**

[1] YOSHIZAWA A., et al., Plasma and Fluid Turbulence, IOP Publishing LtD, 2003
[2] AUSTIN M. E. et. al., Phys Plasmas 13 (2006) 082502
[3] TAKEJI S. et al., Nucl. Fusion 42 (2002) 5;
[4] YU C., et al., Nucl. Fusion **32** (1992) 1545;
[5] JOFFRIN E., et al. Nucl. Fusion **43** (2003) 1167
[6] MCDEVITT C. J., et al., Phys. Plasmas **13** (2006) 032302
[7] ISHIZAWA A., et al., Phys. Plasmas 15 (2008) 084504
[8] MILITELLO F., et al., Phys. Plasmas 15 (2008) 050701
[9] WANG Z. X. et al., Phys. Rev. Letts. **103**, (2009) 015004
[10] Wang Z. X., et al. Phys. Plasmas **16**, 060703(2009)
[11] LI J., et al. Nucl. Fusion 49 (2009) 095007
[12] WILSON H. R., et al., Phys. Plasmas 51 (2009) 115007
[13] MURAGLIA M., et al., Phys. Rev. Letts. 103 (2009) 145001
[14] YAGI M., et al., Nucl. Fusion 45 (2005) 900
[15] WAELBROECK F. L., et al., Phys. Rev. Lett. **78** (1997) 1703
[16] HENDER T. C., et al. Nucl. Fusion **47** (2007) S128
[17] LA HAYE R. J., et al. Nucl. Fusion **32** (1992) 2119(1992)
[18] BUTTERY R. J., et al., Nucl. Fusion **39** (1999) 1827
[19] WESSON J., Tokamaks, 2nd Ed., Clarendon, Oxford (1997)
[20] LI J., et al., Phys. Plasmas **5** (1998) 959
[21] FURTH H. P., et al., Phys. Fluids **6** (1963) 459
[22] LI J. and KISHIMOTO Y., Phys. Plasmas **11 (2004)** 1493
[23] LOUREIRO N. F., et al., Phys. Rev. Lett. **95** (2005) 235003
[24] FITZPATRICK R., Nucl.Fusion **33** (1993) 1049
[25] ROBERTS P. H., et al., Annu. Rev. Fluid Mech. **24** (1992) 459
[26] TOBIAS S. M., Phil. Trans. R. Soc. Lond. A **360** (2002) 2741
[27] ALFVEN H., J. Geophys. Res. **81** (1976) 4019
[28] SCOTT B., et al., Phys. Fluids **28** (1985) 275
[29] OTTAVIANI M., et al., Phys. Rev. Lett. 93 (2004) 075001
[30] CHANG Z., et al. Nucl. Fusion **34** (1994) 1309(1994)
[31] ISAYAMA A., et al., Plasma Phys. Control. Fusion **41** (1999) 35